Transcriptomics: Open Access
ISSN: 2329-8936
Castillo et al., Transcriptomics 2015, 3:2
DOI: 10.4172/2329-8936.1000120
Research Article
Open Access

Gene Expression Profile and Signaling Pathways in MCF-7 Breast Cancer Cells Mediated by Acyl-CoA Synthetase 4 Overexpression

Ana F Castillo#, Ulises D Orlando#, Paula Lopez, Angela R Solano, Paula M. Maloberti and Ernesto J Podesta*

Biomedical Research Institute, Inbiomed, Department of Biochemistry, School of Medicine University of Buenos Aires, CABA, C1121ABG, Argentina
#equally Contributed

Abstract

Aim: Breast cancer comprises a heterogeneous group of diseases that vary in morphology, biology, behavior and response to therapy. Previous studies have identified an acyl-CoA synthetase 4 (ACSL4) gene-expression pattern correlated with very aggressive tumors. In particular, we have used the tetracycline Tet-Off system to stably transfect non-aggressive breast cancer MCF-7 cells and developed a stable line overexpressing ACSL4 (MCF-7 Tet-Off/ACSL4). As a result, we have proven that cell transfection solely with ACSL4 cDNA renders a highly aggressive phenotype *in vitro* and results in the development of growing tumors when injected into nude mice. Nevertheless, and in spite of widespread consensus on the role of ACSL4 in mediating an aggressive phenotype in breast cancer, the early steps through which ACSL4 increases tumor growth and progression have been scarcely described and need further elucidation. For this reason, the goal of this work was to study the gene expression profile and the signaling pathways triggered by ACSL4 overexpression in the mechanism that leads to an aggressive phenotype in breast cancer.

Methods: We have performed a massive in-depth mRNA sequencing approach and a reverse-phase protein array using MCF-7 Tet-Off/ACSL4 cells as a model to identify gene expression and functional proteomic signatures specific to ACSL4 overexpression.

Results and Conclusion: The sole expression of ACSL4 displays a distinctive transcriptome and functional proteomic profile. Furthermore, gene networks most significantly upregulated in breast cancer cells overexpressing ACSL4 are associated to the regulation of embryonic and tissue development, cellular movement and DNA replication and repair. In conclusion, ACSL4 is an upstream regulator of tumorigenic pathways. Because an aggressive tumor phenotype appears in the early stages of metastatic progression, the previously unknown mediators of ACSL4 might become valuable prognostic tools or therapeutic targets in breast cancer.

Keywords: Acyl-CoA synthetase 4; Gene signature; Transcriptome; Functional proteomics; Breast cancer

Introduction

Breast cancer remains the second most important cause of death (by cancer) among women [1]. Patients who cannot be cured are those in whom breast cancer has metastasized, that is, breast cancer cells have migrated and invaded other organs such as lung and bone. As no effective therapies are currently available, aggressive breast cancer constitutes a key field for both researchers and clinicians. It has been shown that both in breast cancer cell lines and in tumor samples the expression of acyl-CoA synthetase 4 (ACSL4) is directly correlated with aggressiveness in breast cancer and inversely correlated with estrogen receptor alpha (ERα) levels [2-4]. ACSL4 belongs to a five-member family of enzymes that esterifies mainly arachidonic acid (AA) into acyl-CoA [2-5]. Unlike the other ACSL isoforms, ACSL4 is encoded on the X chromosome and its expression is highest in adrenal cortex, ovary and testis [6-10], as well as in mouse and human cerebellum and hippocampus [11]. Studies on the physiological functions of ACSL4 have revealed possible roles in polyunsaturated fatty acid metabolism in brain, in steroidogenesis, in eicosanoid metabolism related to apoptosis and embryogenesis [8-14]. ACSL4 expression has also been associated with non-physiological functions such as mental retardation disorder [15,16] and cancer [2,3,17,18]. ACSL4 was first associated with cancer due to its abnormal expression in colon and hepatocellular carcinoma. Increased ACSL4 expression, both at mRNA and protein levels [18], in colon adenocarcinoma cells has been associated with the inhibition of apoptosis and an increase in cell proliferation when compared to adjacent normal tissue. ACSL4 has also been suggested as a predictive factor for drug resistance in breast cancer patients receiving adriamycin-containing chemotherapy [19]. We have demonstrated a positive correlation of ACSL4 expression and aggressiveness in breast cancer cell lines, with the highest expression found in metastatic lines derived from triple-negative tumor breast cancer (MDA-MB-231 and Hs578T) [3]. Functionally, we have found that ACSL4 is part of the mechanism responsible for increased breast cancer cell proliferation, invasion and migration, both *in vitro* and *in vivo* [3,4]. We have further demonstrated that ACSL4 can be silenced to reduce cell line aggressiveness. The role of ACSL4 in the development of growing tumors found further support when tumor growth was inhibited through the inhibition of ACSL4 expression [5]. However, even if the role of ACSL4 in mediating an aggressive phenotype in breast cancer is well accepted, its underlying mechanisms have been scarcely explored. For this reason, the goal of this work was to study the gene expression profile and the signaling pathways triggered by ACSL4 overexpression in the mechanism that leads to an aggressive phenotype in breast cancer. Thus, we have performed a massive in-depth mRNA sequencing approach and a reverse-phase protein array using ACSL4-overexpressing MCF-7 cells, as a model to identify gene expression and functional proteomic signatures specific to ACSL4 overexpression.

Materials and Methods

Cell culture

The human breast cancer cell line was generously provided by Dr.

***Corresponding author:** Ernesto J Podesta, Biomedical Research Institute, Inbiomed, Department of Biochemistry, School of Medicine University of Buenos Aires, CABA, C1121ABG, Argentina, Tel: 541149644027; E-mail: ernestopodesta@yahoo.com.ar

Received October 23, 2015; **Accepted** November 20, 2015; **Published** November 23, 2015

Citation: Castillo AF, Orlando UD, Lopez P, Solano AR, Maloberti PM, et al. (2015) Gene Expression Profile and Signaling Pathways in MCF-7 Breast Cancer Cells Mediated by Acyl-CoA Synthetase 4 Overexpression. Transcriptomics 3: 120. doi:10.4172/2329-8936.1000120

Vasilios Papadopoulos (Research Institute of the McGill University Health Centre, Montreal, Canada) and obtained from the Lombardi Comprehensive Cancer Center (Georgetown University Medical Center, Washington D.C., USA). The tetracycline-repressible MCF-7 cell lines, designated MCF-7 Tet-Off empty vector, and MCF-7 Tet-Off-induced repression of ACSL4, designated MCF-7 Tet-Off/ACSL4, were obtained previously in the laboratory [3]. The cell lines were maintained in Dulbecco's modified Eagle (DMEM) medium (GIBCO, Invitrogen Corporation,Grand Island, NY, USA) supplemented with 10% Fetal calf serum (PAA laboratories GmbH, Pasching, Austria) plus 100 U/ml penicillin and 10 mg/ml streptomycin (GIBCO, Invitrogen Corporation,Grand Island, NY, USA). Doxycycline (Sigma Chemical Co.,St. Louis, MO, USA), a more stable tetracycline analogue, was used to regulate the expression of the Tet-Off system. Sterile and plastic material for tissue culture was from Orange Scientific (Braine-l'Alleud, Belgium). All other reagents were of the highest grade available.

RNA-Seq sample preparation and sequencing

For each cell line, total RNA was extracted by Direct-zol RNA kit (Zymo Research, Irvine, CA, USA). RNA quality was assessed by agarose gel electrophoresis (visual absence of significant 28S and 18S rRNA degradation) and by spectrophotometry. RNA-Seq was performed by Zymo Research facility performing PolyA enrichment of the RNA samples. HiSeq 2 x 50 bp paired-ends reads from RNA-Seq of a human normal-tumor pair samples were analyzed first using the TopHat and Cufflinks software. TopHat (v2.0.6) was utilized for alignment of short reads to GRCh37, Cufflinks (v2.0.2) for isoform assembly and quantification, and commeRbund (v2.0.0) for visualization of differential analysis. Default parameters were used. The RNA-Seq quality control was performed using Dispersion, Volcano, MA, Density, PCA, Scatter and Box plots.

Quantitative reverse transcription-PCR (qRT-PCR)

MCF-7 Tet-Off empty vector and MCF-7 Tet-Off/ACSL4 total RNA was extracted using Tri-Reagent (Molecular Research Center, Cincinnati, OH, USA) following the manufacturer's instructions. Any residual genomic DNA was removed by treating RNA with DNase I (Invitrogen, Carlsbad, CA, USA) at room temperature for 15 min, which was subsequently inactivated by incubation with 2.5 mM EDTA for 10 min at 65°C. Two µg of total RNA were reverse transcribed using random hexamers and M-MLV Reverse Transcriptase (Promega, Madison, WI, USA) according to the manufacturer's protocol. For real-time PCR, gene specific primers were obtained from RealTimePrimers.com (Elkins Park, PA, USA). Real-time PCR was performed using Applied Biosystems 7300 Real-Time PCR System and 20 µl of a solution containing 5 µl of cDNA, 10 µM forward and reverse primers, and 10 µl of SYBR Select Master Mix (Applied Biosystems, Carlsbad, CA, USA) for each reaction. All reactions were performed in triplicate. Amplification was initiated by a 2-min preincubation at 50°C, 2-min incubation at 95°C, followed by 40 cycles at 95°C for 15 sec, 55°C for 15 sec and 72°C for 1 min, terminating at 95°C for the last 15 sec. Gene mRNA expression levels were normalized to human 18S RNA expression, performed in parallel as endogenous control. Real-time PCR data were analyzed by calculating the $2^{-\Delta\Delta Ct}$ value (comparative Ct method) for each experimental sample.

David and Ingenuity Pathways Analysis

To identify the statistically significant biological functions and signaling pathways affected by the genes differentially expressed in our comparisons, we used Database for Annotation, Visualization and Integrated Discovery (DAVID) [20] and Ingenuity Pathways Analysis (IPA; Ingenuity Systems, Inc., Cambridge, MA, USA) [21]. IPA is the largest curated database and analysis system for understanding the signaling and metabolic pathways, molecular networks and biological processes that are most significantly changed in a dataset of interest. Ranking and significance of the biofunctions and the canonical pathways were tested by the *p*-value. Additionally, canonical pathways were ordered by the ratio (number of genes from the input data set that map to the pathway divided by the total number of molecules that exist in the canonical pathway). IPA also generated cellular networks where the differentially regulated genes were related according to previously known associations between genes or proteins, but independently of established canonical pathways. Top networks represent associative network functions based on a score that considers the –log (*p*-value), which aggregates the likelihood that genes in the network are found together due to random chance.

Reverse phase protein assay (RPPA)

RPPA was performed in the RPPA Core Facility - Functional Proteomics from MD –Anderson Cancer Center, University of Texas, TX, USA. Cellular proteins were denatured by 1% SDS (with beta-mercaptoethanol) and diluted in five 2-fold serial dilutions in dilution buffer (lysis buffer containing 1% SDS). Serial diluted lysates were arrayed on nitrocellulose-coated slides (Grace Biolab) by Aushon 2470 Arrayer (Aushon BioSystems) [22].

Statistical Analysis

Data analysis was performed using GraphPad InStat Software 3.01 (La Jolla, CA, USA). Statistical significance was determined by analysis of variance (ANOVA) followed by Tukey- Kramer Multiple Comparison Test and Spearman's rank correlation coefficient was calculated using Social Science Statistics free statistics software.

Results and Discussion

Differential gene expression triggered by ACSL4

As ACSL4 plays a crucial role in tumor growth, we have undertaken a systematic study to identify genes with tumorigenesis capacity and elucidate the underlying signaling mechanism. Toward understanding the capacity of ACSL4 in the regulation of tumorigenesis, we have previously reported the involvement of AA lipoxygenase and cyclooxygenase metabolites in the action of ACSL4 [3,4] and, in this report, we focus on the identification of ACSL4-responsive genes using the RNA-Seq in MCF-7 Tet-Off/ACSL4 compared with an MCF-7 Tet-Off empty vector. This system is particularly valuable in enabling both the overexpression and the specific inhibition of ACSL4 through doxycycline treatment and has been previously used to develop tumors in xenograft models [3,4]. Results show a total of 26705366 RNA-Seq reads acquired from MCF-7 Tet-Off/ACSL4 and 22258811 reads acquired from MCF-7 Tet-Off empty vector. We next aligned the sequence reads to a human genome reference (GRCh37) using TopHat version 2.0.6, with results rendering 93.30% of the MCF-7 Tet-Off/ACSL4 reads and 92.90% of the MCF-7 Tet-Off empty vector reads as successfully mapped. The resulting read alignments (file format: BAM) were then assembled through Cufflinks version 2.0.2 for isoform assembly and quantification, and commeRbund (v2.0.0) for visualization of differential analysis (default parameters were used). The RNA-Seq quality control was performed using Dispersion, Volcano, MA, Density, PCA, Scatter and Box plots. Gene expression levels were determined by measuring the sum of fragments per kilobase of exon model per million of reads mapped (FPKM), analyzed in each exon. To acquire more accurate results, data were filtered out whenever

estimated FPKM values in both MCF-7 Tet-Off/ACSL4 and MCF-7 Tet-Off empty vector samples were less than 1.0 (cf. an FPKM value of 0.05 is commonly set as the lowest boundary of expression level). Only loci having a $\log_2$ (fold change) > 2 between MCF-7 Tet-Off/ACSL4 and MCF-7 Tet-Off empty vector were considered. Ultimately, we observed that, from 32247 successfully sequenced loci, 3944 were significantly and differentially expressed in MCF-7 Tet-Off/ACSL4 samples. Among them, 2501 were upregulated and 1443 were downregulated. ACSL4 gene was one of the genes taken as a control of its overexpression and, as expected, it was one of the genes showing major differences between MCF-7 Tet-Off/ACSL4 and MCF-7 Tet-Off empty vector. Table 1 shows the top genes which exhibit differential changes when ACSL4 is overexpressed. To determine the characteristic chromosomal location of genes controlled by ACSL4 expression, we used the CROC program [23] to examine the expression landscape by plotting the number of differentially expressed genes along the whole chromosomes. Results revealed that chromosome distribution patterns varied greatly with respect to gene density and, in particular, chromosome 1 showed the highest gene density among genes mapped (Figure S1). A total of 52 clusters were found –chromosome 1 showed the highest number of clusters (8)-, while the number of genes in clusters was 181.

Enriched functional categories of gene networks relating to the transcripts regulated by ACSL4 overexpression

To gain insights into biological cell properties, IPA was used to rank enriched functional categories of gene networks relating to the transcripts regulated in ACSL4-responsive gene sets acquired from the RNA-Seq data. The highest-scoring associated diseases and disorders are shown in Table 2, while cancer was the disease showing the lowest *p*-value among diseases and disorders. As a result, we verified 390 top biofunctions concerned with the ACSL4-induced transcriptome alteration in MCF-7 Tet-Off/ACSL4 cells. The most significantly tumorigenesis-related biofunctions (only *p*-values under 0.01) are shown in Table 3. In agreement with our previous results regarding ACSL4 effect on cell proliferation, invasion and migration [3,4], the top three biofunctions which were IPA-predicted to be increased in RNA-Seq data were cell movement migration and proliferation. Table S1 shows a detailed list of molecules altered in these biofunctions. Table 4 shows the top ten most significantly upregulated functions related to gene networks in the RNA-Seq –along with a list of the corresponding genes in each function network–, while Figure S2 shows the network corresponding to the top ten upregulated functions. DNA replication,

GENES UPREGULATED				
Name	**Gene Symbol**	**Location**	**Type(s)**	**$\log_2$ fold change**
NADPH oxidase 3	*NOX3*	cytoplasm	enzyme	13.21
De-etiolated homolog 1 (Arabidopsis)	*DET1*	nucleus	other	10.97
Patched 2	*PTCH2*	plasma membrane	transmembrane receptor	10.9
Wingless-type MMTV integration site family, member 6	*WNT6*	extracellular space	other	6.74
Zinc finger, matrin-type 4	*ZMAT4*	nucleus	other	5.02
Retinoic acid induced 2	*RAI2*	unknown	other	4.75
Dual specificity phosphatase 18	*DUSP18*	cytoplasm	phosphatase	4.69
Transcription factor B1, mitochondrial	*TFB1M*	cytoplasm	transcription regulator	4.58
MAP/microtubule affinity-regulating kinase 1	*MARK1*	cytoplasm	kinase	4.30
Interleukin 20	*IL20*	extracellular space	cytokine	4.29
Fatty acyl CoA reductase 2	*FAR2*	cytoplasm	enzyme	4.16
Ets homologous factor	*EHF*	nucleus	transcription regulator	4.09
SH3-domain GRB2-like 3	*SH3GL3*	cytoplasm	other	4.06
2'-5'-oligoadenylate synthetase 1, 40/46kDa	*OAS1*	cytoplasm	enzyme	4.05
Synaptotagmin XIII	*SYT13*	plasma membrane	transporter	3.85
Aldehyde oxidase 1	*AOX1*	cytoplasm	enzyme	3.78
G protein, alpha inhibiting activity	*GNAI1*	plasma membrane	enzyme	3.78
FXYD domain containing ion transport regulator 5	*FXYD5*	plasma membrane	ion channel	3.75
Cytochrome c oxidase subunit VIIb2	*COX7B2*	unknown	unknown	3.73
Wingless-type MMTV integration site family, member 10A	*WNT10A*	extracellular space	other	3.60
Interferon, alpha-inducible protein 6	*IFI6*	cytoplasm	other	3.35
Sp6 transcription factor	*SP6*	nucleus	transcription regulator	3.35
Acyl-CoA oxidase 2, branched chain	*ACOX2*	cytoplasm	enzyme	3.31
Transforming growth factor, beta 2	*TGFB2*	extracellular space	growth factor	3.22
Interleukin 24	*IL24*	extracellular space	cytokine	3.15
GABA(A) receptor-associated protein like 1	*GABARAPL1*	cytoplasm	other	2.54
FBJ murine osteosarcoma viral oncogene homolog	*FOS*	nucleus	transcription regulator	2.41
Laminin, beta 1	*LAMB1*	extracellular space	other	2.37
Nuclear receptor coactivator 4	*NCOA4*	nucleus	transcription regulator	2.09
Phospholipase D1, phosphatidylcholine-specific	*PLD1*	cytoplasm	enzyme	2.09
v-Erb-b2	*ERBB2*	plasma membrane	kinase	2.05
Fibroblast growth factor 11	*FGF11*	extracellular space	other	2.04
Ret proto-oncogene	*RET*	plasma membrane	kinase	2.04
Fibroblast growth factor receptor 1	*FGFR1*	plasma membrane	kinase	2.04
Integrin, alpha 2 (CD49B, alpha 2 subunit of VLA-2 receptor)	*ITGA2*	plasma membrane	transmembrane receptor	2.02
Eukaryotic translation initiation factor 2-alpha kinase 2	*EIF2AK2*	cytoplasm	kinase	1.94
Unc-51 like autophagy activating kinase 1	*ULK1*	cytoplasm	kinase	1.83
Vascular endothelial growth factor A	*VEGFA*	extracellular space	group	1.75

GENES DOWNREGULATED				
Name	**Gene Symbol**	**Location**	**Type(s)**	**log_2 fold change**
Protein tyrosine phosphatase, non-receptor type 22	*PTPN22*	cytoplasm	phosphatase	-11.55
ADAM metallopeptidase with thrombospondin type 1 motif, 9	*ADAMTS9*	extracellular space	peptidase	-11.21
Prickle homolog 2	*PRICKLE2*	nucleus	other	-11.08
Neurotrophic tyrosine kinase, receptor, type 3	*NTRK3*	plasma membrane	kinase	-8.13
Contactin associated protein-like 3B	*CNTNAP3B*	unknown	other	-7.29
WNT inhibitory factor 1	*WIF1*	extracellular space	other	-4.75
Keratin, Type I cytoskeletal 20	*CK20 (KRT20)*	cytoplasm	other	-4.22
Deiodinase, iodothyronine, type II	*DIO2*	cytoplasm	enzyme	-3.62
Zinc finger protein 217	*ZNF217*	nucleus	transcription regulator	-3.41
Ca^{++}-dependent secretion activator	*CADPS*	plasma membrane	other	-3.15

Table 1: Identification of significantly upregulated and downregulated genes by ACSL4 overexpression using RNA-Seq.

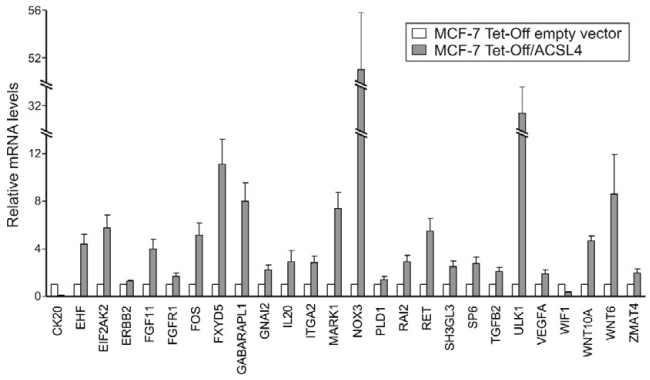

Figure 1: Real-time RT-PCR analysis of the top genes exhibiting differential changes in RNA-Seq when ACSL4 is overexpressed. Total RNA was isolated from MCF-7 Tet-Off empty vector and MCF-7 Tet-Off/ACSL4 cells, reverse transcribed and subjected to real-time PCR using specific primers. Each transcript expression level was normalized to human 18S RNA expression, performed in parallel as endogenous control. Real-time PCR data were analyzed by calculating the $2^{-\Delta\Delta Ct}$ value (comparative Ct method) for each experimental sample. Relative mRNA expression levels are shown. Data are presented as mean ± standard deviation (SD).

Name of Diseases and Disorders	***p*-value**	**# molecules**
Cancer	5.74E-07 - 0.0191	530
Infectious Disease	4.56E-05 - 0.0174	136
Reproductive System Disease	7.35E-05 -1.87E-02	163
Dermatological Diseases and Conditions	8.42E-05 - 0.0141	74
Endocrine System Disorders	1.09E-04 - 0.0197	78

Table 2: Top associated diseases and disorders analyzed by IPA. Top significantly diseases and disorders concerned with the ACSL4-induced transcriptome alteration in MCF-7 Tet-Off/ACSL4 cells.

Category	**Diseases or Functions Annotation**	***p*-value**	**Predicted Activation State**	**Activation z-score**	**# Molecules**
Cellular Movement	cell movement	3.97E-07	Increased	4.685	182
Cellular Movement	migration of cells	4.65E-07	Increased	4.677	166
Cellular Growth and Proliferation	proliferation of cells	2.04E-06	Increased	2.390	295
Cellular Assembly and Organization	formation of cellular protrusions	7.15E-05	Increased	3.830	73
Cellular Assembly and Organization	microtubule dynamics	1.48E-04	Increased	4.169	94
Cellular Assembly and Organization	organization of cytoskeleton	1.89E-04	Increased	3.662	107
Gene Expression	transactivation	3.17E-04	Increased	3.318	59
Cellular Assembly and Organization	organization of cytoplasm	3.73E-04	Increased	3.714	113
Carbohydrate Metabolism	sulfation of polysaccharide	4.39E-04	Increased	2.132	5
Gene Expression	transactivation of RNA	9.23E-04	Increased	3.718	54
Cancer	proliferation of cancer cells	1.05E-03	Increased	2.009	37
Cellular Assembly and Organization	formation of plasma membrane projections	1.20E-03	Increased	2.128	49
Cellular Growth and Proliferation	proliferation of connective tissue cells	1.45E-03	Increased	2.628	54
Cellular Development	branching of cells	1.60E-03	Increased	3.043	17
Cellular Movement	cell movement of tumor cell lines	2.20E-03	Increased	2.034	67
Cellular Movement	migration of tumor cell lines	2.26E-03	Increased	2.139	55
Cellular Movement	cell movement of tumor cells	2.41E-03	Increased	2.530	19
Cell Morphology	shape change of tumor cell lines	5.81E-03	Increased	2.180	16
Cellular Development	differentiation of stem cells	8.78E-03	Increased	2.540	21
Cancer	prostate cancer and tumors	1.17E-02	Increased	2.200	54
Cellular Assembly and Organization	growth of plasma membrane projections	1.18E-02	Increased	2.866	40
Cellular Movement	migration of tumor cells	1.26E-02	Increased	2.089	20
Cell Morphology	shape change of neurons	1.26E-02	Increased	2.205	6

Table 3: Top associated biofunctions by IPA. Top significantly tumorigenesis-related biofunctions concerned with the ACSL4-induced transcriptome alteration in MCF-7 Tet-Off/ACSL4 cells. Only *p*-values under 0.01 calculated by right-tailed Fisher's Exact test were considered significant. IPA uses the activation z-score algorithm to make predictions. The z-score algorithm is designed to reduce the chance that random data will generate significant predictions.

Network	Score	Focus Molecules	Top Diseases and Functions	Molecules in Network
1	44	33	DNA Replication, Recombination, and Repair, Gene Expression, Cancer	*CALCOCO1, CBX2, CBX5, CBX8, CHRNE, DIAPH2, ELF5, HIST1H3A (includes others), HIST1H4A (includes others), HIST2H2AA3/HIST2H2AA4, HIST2H2AC, HIST2H2BE (includes others), HIST2H3C (includes others), HIST3H2A, HOXD8, IL20, IL17R, IL17RC, KLF11, MSL3, MSMB, MT1G, NEK3, PARP10, RCC1, S100A7, SCML1, SHISA2, TEAD4, TFAP2C, TRANK1, TTC1, Vegf, WDR61, ZNF324B*
2	43	32	Carbohydrate Metabolism, Small Molecule Biochemistry, Post-Translational Modification	*A4GALT, ATL1, B4GALT1, B4GALT5, B4GALT6, B4GALT7, CDC42EP5, CMTM8, CYP4Z1, DSC2, EMCN, ERK1/2, ETV4, FAIM3, Galactosyltransferase beta 1, 4, GLIPR2, HS6ST2, KLF13, LINGO1, LRRN1, MMD, MUC5B, NDST1, NMU, OLFM1, PKP2, RAPGEF2, RTKN, RTN4R, RTN4RL2, SHC4, ST6GAL1, sulfotransferase, TP53TG1, ZNF217*
3	35	28	Molecular Transport, Hereditary Disorder, Neurological Disease	*ANO3, AP-3, AP3B2, AP3D1, ATP6V0A4, ATP6V0B, ATP6V1C2, CBR3, DOK3, EDARADD, EHF, ENO3, FBXO41, H+-exporting ATPase, H+-transporting two sector ATPase, KCND3, MIB2, MTORC1, NFIX, NFkB (complex), PDCD11, PGM1, PNKD, PRMT2, PRPH, RFTN1, S100, S100A1, S100P, SGCB, SGCG, TFEB, TMOD2, Vacuolar H+ ATPase, ZNF385A*
4	31	26	Cellular Development, Embryonic Development, Developmental Disorder	*ADAMTS9, ADCY, ADCY6, AGPAT9, Angiotensin II receptor type 1, BIK, C8orf4, CAPN8, DGAT2, EYA2, Fascin, FATE1, FSCN2, GABRB3, GGT5, GNAI1, HOXA5, INSIG2, IRS, Nr1h, NUCB1, p70 S6k, PADI2, PDE4D, PDE4DIP, Pkc(s), PODXL, PSCA, RGS6, SIX2, SLC1A1, SOCS, SP110, TPM2, TSH*
5	31	26	Cardiovascular Disease, Cancer, Dermatological Diseases and Conditions	*ABCC8, ABLIM1, ABLIM2, CCNG2, CRAT, DEAF1, DLX4, FOXO4, GATA6, GPX2, GUCY1A3, Hedgehog, Histone h4, ID3, KLF2, LMO2, Notch, NOTCH2, PI3K (family), PLEKHF1, PTCH1, PTCH2, QPCT, Ras, RCN1, Secretase gamma, SLC26A2, SMAD6, SMOOTH MUSCLE ACTIN, TAGLN, TCF, TNNT1, TOB2, ZC3H15*
6	31	26	Carbohydrate Metabolism, Tissue Morphology, Ophthalmic Disease	*ACAA2, Alpha catenin, BMP7, BRSK1, BSG, CBR4, CDH8, CHST11, CLDN23, CNKSR3, collagen, Collagen(s), CTGF, elastase, ERBB2, estrogen receptor, FAM134B, GJB3, HSD17B, HSD17B7, HSD17B8, HSD17B14, Integrin, KIFC3, MAP2K1/2, Mmp, MMP23B, PLEK2, PRR15L, RNF149, SOWAHC, SOX4, SYNPO, TSPAN4, ZNF703*
7	29	25	Cell Morphology, Hair and Skin Development and Function, Organ Morphology	*ACHE, Akt, ANTXR1, ARHGAP24, ASAH2, CHCHD2, chymotrypsin, COL18A1, COL6A2, Collagen type IV, Collagen type VI, CSF2RA, EPHB4, gelatinase, GPIIB-IIIA, GSTZ1, ITGA2, ITGB4, LAMB1, Laminin, Laminin1, MEX3B, MGLL, mir-29, MSR1, PID1, PPT1, PTTG1IP, RAP1GAP, SCARA3, SCAVENGER receptor CLASS A, STARD13, TACSTD2, TNFRSF21, Vla-4*
8	29	25	Cell Morphology, Cellular Compromise, Lipid Metabolism	*Alpha Actinin, Alpha tubulin, Ant, ARL2BP, ASCL2, ASIC3, Beta Tubulin, calpain, CLINT1, DCDC2, DHRS2, DMTN, DPYSL2, ESPN, F Actin, FMNL1, Focal adhesion kinase, GABARAPL1, MARCKS, Mucin, PACSIN1, SHROOM3, SLC25A4, SLC25A6, SNX33, Spectrin, STOM, Talin, TBC1D2B, TOMM20L, TPT1, TRDMT1, TSPO, VDAC1, WAS*
9	29	25	Cancer, Dermatological Diseases and Conditions, Hematological Disease	*60S ribosomal subunit, ANKRD13B, ATR, CCDC22, CCDC53, CCDC93, CKB, COL11A2, Collagen type II, CTSL, DNAJC27, Dynamin, E2F8, ENaC, ERRFI1, FAM21A/FAM21C, HSP, Hsp27, Hsp70, HSPA8, let-7, mGluR, NXT2, OPTN, p85 (pik3r), RPL39, RPLP1, RRM2, SH3GL3, TM4SF1, TNRC6C, TRPC1, Ubiquitin, UCHL1, ZNF219*
10	29	25	Endocrine System Development and Function, Small Molecule Biochemistry, Developmental Disorder	*ACPP, ACSS1, ADRB, AGBL2, ATP9A, BOK, C8G, CA4, Cg, CHST8, Creb, DIO2, EPHB6, FAM198B, FAM214A, FSH, Igm, KHDRBS3, Lh, LIMCH1, MAMLD1, Mek, OGFR, ONECUT1, PLC, PTPN21, PTTG1, RAB33B, Raf, Rap1, RETSAT, SGSM2, SLCO4A1, TP53I11, YPEL3*

Table 4: Gene networks of ACSL4-overexpressing cells. RNA-Seq data were analyzed for significantly regulated functions using IPA. The genes associated with each function network shown in the last column are significantly regulated in the ACSL4-overexpressing cells. Score: negative exponent of *p*-value calculated by a right-tailed Fisher's Exact test, which calculates the likelihood that network eligible molecules are found together by random chance alone.

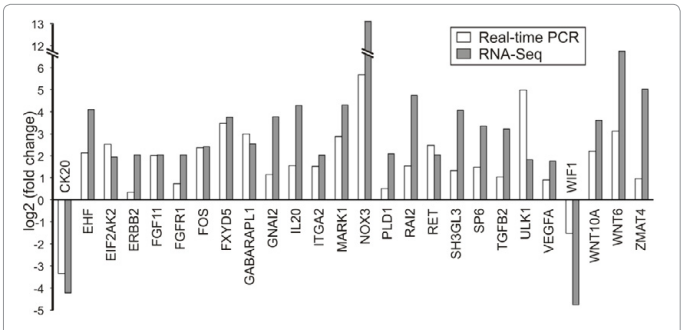

Figure 2: Validation of RNA-Seq data. Correlation between RNA-Seq and real-time PCR data of differential gene expression from MCF-7 Tet-Off/ACSL4 to MCF-7 Tet-Off empty vector cells. Data are presented as $\log_2$ ratios. Spearman's rank correlation coefficient was 0.55525 and the two-tailed value of *p* was 0.00001. By normal standards, the positive correlation between the two variables would be considered statistically significant.

recombination, repair, gene expression and cancer showed the highest score. In particular, the finding that cellular development and embryogenesis are within the top ten biofunctions is interestingly in agreement with recent work showing the crucial role of ACSL4 pathways in embryo development in zebrafish [12] and Drosophila [14,24].

RNA-Seq data confirmed by analysis of gene expression changes by real-time RT-PCR

We further validated the gene expression changes found in RNA-Seq data and IPA by real-time RT-PCR in independent biologic repeats of samples from MCF-7 Tet-Off/ACSL4 and MCF-7 Tet-Off empty vector under the same conditions used for RNA-Seq analysis (relative mRNA expression levels are shown in (Figure 1). A comparison of fold changes between RNA-Seq and real-time RT-PCR for each gene is shown in Figure 2, which verifies that the real-time RT-PCR expression profiles were mostly in agreement with RNA-Seq data. Although there were small differences in the fold change values between the two methods of measurement, results were generally highly related (Spearman's rank correlation coefficient was 0.55525 and the two-tailed value of *p* was 0.00001) strongly supporting the reliability of our RNA-Seq analysis. We next focused our attention on categories that were relevant to this study, subgrouped these genes by function and measured an example of each of them (i.e. cytokines, transcription factors, growth factors, integrin family and cytoskeleton, Wnt signaling family, oncogenes, growth factor receptors and energy metabolism). Most of these genes have central roles in the biology of cancer cells regarding proliferation, migration and invasion. ACSL4 increased the

expression levels of interleukin 20 *IL20*, Ets homologous factor (*EHT*), SP6 transcription factor (Krueppel-like factor 14 or *SP6*), transforming growth factor beta 2 (*TGFβ2*), V-erb avian erythroblastic leukemia viral oncogene homologue 2 (*ERBB2*), vascular endothelial growth factor A (*VEFGA*), integrin alpha 2 (*ITGA2*), MAP/Microtubule affinity-regulating kinase 1 (*MARK1*), FXYD domain containing ion transport regulator 5 (*FXYD5*), ret proto-oncogen (*RET*), murine oesteosarcoma viral oncogene homolog (*FOS*), fibroblast growth factor receptor 1 (*FGFR1*) and Wingless-Type MMTV Integration Site Family Member 6 (*WNT6*) and *WNT10A*. One of the genes showing a marked decrease after ACSL4 expression was the WNT inhibitory factor 1 (*WIF1*). *IL20* has been demonstrated to be upregulated in muscle-invasive bladder cancer patients, while *EHT* and *SP6* are involved in differentiation and carcinogenesis. The SP6 has also been proposed to contribute to the malignant phenotype of breast tumors. *TGFβ2*, *ERbB2*, *VEFGA*, *ITGA2*, *MARK1*, *FXYD5*, *RET* and *FOS* are involved in tumor progression as well. Other genes measured included the Unc-51-like autophagy-activating kinase 1 (*ULK1*) and the retinoic acid induced 2 (*RAI2*). In short, most of the genes confirmed to be upregulated here have well established roles in tumorigenesis. In addition, Table 5 shows the top small nuclear RNA and microRNA (miR) regulated by ACSL4. MicroRNAs play an important role in virtually all biological pathways and they may hence influence numerous cancer-relevant processes. ACSL4 upregulates *miR-29a*, whose overexpression has been described to increase tube formation and migration in endothelial cultures. Mechanistically, *miR-29a* directly targets the phosphatase and tensin homolog (*PTEN*) in endothelial cells, leading to the activation of the AKT pathway [25]. *miR let-7*, an ACSL4-downregulated miR, represses cell proliferation pathways in human cells and has been described as a master regulator of cell proliferation pathways [26]. Overall, the RNA-Seq and IPA have identified genes that could potentially play important roles in the regulation of invasion and migration of breast tumor cells *in vivo*. We further studied enriched canonical pathways and analyzed them through IPA on the basis of RNA-Seq data. Eukaryotic translation initiation factor 2 (EIF2), protein ubiquitination, ribosomal protein S6 kinase 70kDa polypeptide 1 (p70S6K), mechanistic target of rapamycin (mTOR) and the signaling of molecular mechanisms of cancer are among the top canonical pathways triggered by ACSL4 with the lowest *p*-values.

Signal transduction pathways triggered by ACSL4 overexpression

In order to study the signaling pathway triggered by ACSL4 on the basis of RNA-Seq bioinformatic studies, we next defined a functional protein signature of the ACSL4 pathway by using RPPA, a high-throughput antibody-based technique developed for functional proteomic studies to measure phosphorylation states, as well as total levels of key signaling pathway intermediaries. This RPPA used 217 different antibodies directed to signaling proteins or directed to specific phosphorylated sites known to regulate protein signaling activity [22]. The analysis was performed on lysates derived from MCF-7 Tet-Off/ACSL4, MCF-7 Tet-Off empty vector and doxycycline-treated MCF-7 Tet-Off/ACSL4 cells, the latter used to specifically override ACSL4 expression. The pattern of protein expression and/or phosphorylation was remarkably different between MCF-7 Tet-Off/ACSL4 and MCF-7 Tet-Off empty vector. Lysates from doxycycline-treated MCF-7 Tet-Off/ACSL4 cells showed a pattern similar to that of MCF-7 Tet-Off empty vector, further supporting the role of ACSL4 in the effects observed. Figures 3 and 4 show the proteins that exhibited a significant increase or decrease, respectively, in expression or phosphorylation status. ACSL4 overexpression in MCF-7 breast cancer cells changed the pattern of expression or the pattern of phospho-dephosphorylation of about fifty proteins. These effects were reversed by doxycycline treatment, which confirms the specificity of the functional proteomic signature of ACSL4. We next performed a functional annotation analysis using the bioinformatic program DAVID on the basis of RPPA data Figure 5 shows the DAVID scheme of pathways in cancer. ACSL4 overexpression stimulated the dephosphorylation of two proteins and the phosphorylation of thirteen proteins, among which it markedly

Small nuclear RNA (some examples)	Gene Symbol	Location	Change
RNA, U12 small nuclear	*RNU12*	Nucleus	Upregulated
RNA, U4 small nuclear 1	*RNU4-1*	Nucleus	Upregulated
RNA, U4atac small nuclear (U12-dependent splicing)	*RNU4ATAC*	Nucleus	Upregulated
RNA, U5A small nuclear 1	*RNU5A-1*	unknown	Upregulated
RNA, U5D small nuclear 1	*RNU5D-1*	unknown	Upregulated
RNA, U5E small nuclear 1	*RNU5E-1*	unknown	Upregulated
small nucleolar RNA, H/ACA box 8	*SNORA4*	unknown	Downregulated
Micro RNA (some examples)	**Gene Symbol**	**Location**	**Change**
microRNA 29a	*miR-29*	Cytoplasm	Upregulated
microRNA 1290	*miR-1290*	Cytoplasm	Upregulated
microRNA 25	*miR-25*	Cytoplasm	Downregulated
microRNA let-7a-1	*let-7*	Cytoplasm	Downregulated
microRNA let-7d	*let-7*	Cytoplasm	Downregulated

Table 5: Top small nuclear RNA and microRNA regulated by ACSL4.

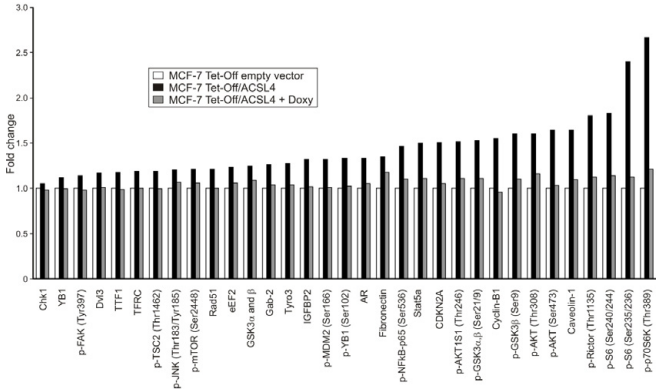

Figure 3: Identification of significantly upregulated protein expression or phosphorylation in ACSL4-overexpressing cells using RPPA. Proteins were extracted from MCF-7 Tet-Off empty vector, MCF-7 Tet-Off/ACSL4 cells and doxycycline treated-MCF-7 Tet-Off/ACSL4 (Doxy, 1 ug/ml, 48 h) cells, and were subjected to RPPA analysis. Data are presented as fold changes (only results with *p*-values under 0.05 are shown).

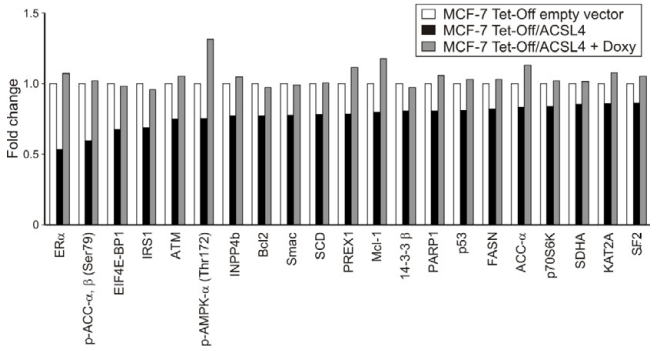

Figure 4: Identification of significantly downregulated protein expression or phosphorylation in ACSL4-overexpressing cells using RPPA. Proteins were extracted from MCF-7 Tet-Off empty vector, MCF-7 Tet-Off/ACSL4 cells and doxycycline treated-MCF-7 Tet-Off/ACSL4 (Doxy, 1 ug/ml, 48 h) cells, and were subjected to RPPA analysis. Data are presented as fold changes (only results with *p*-values under 0.05 are shown).

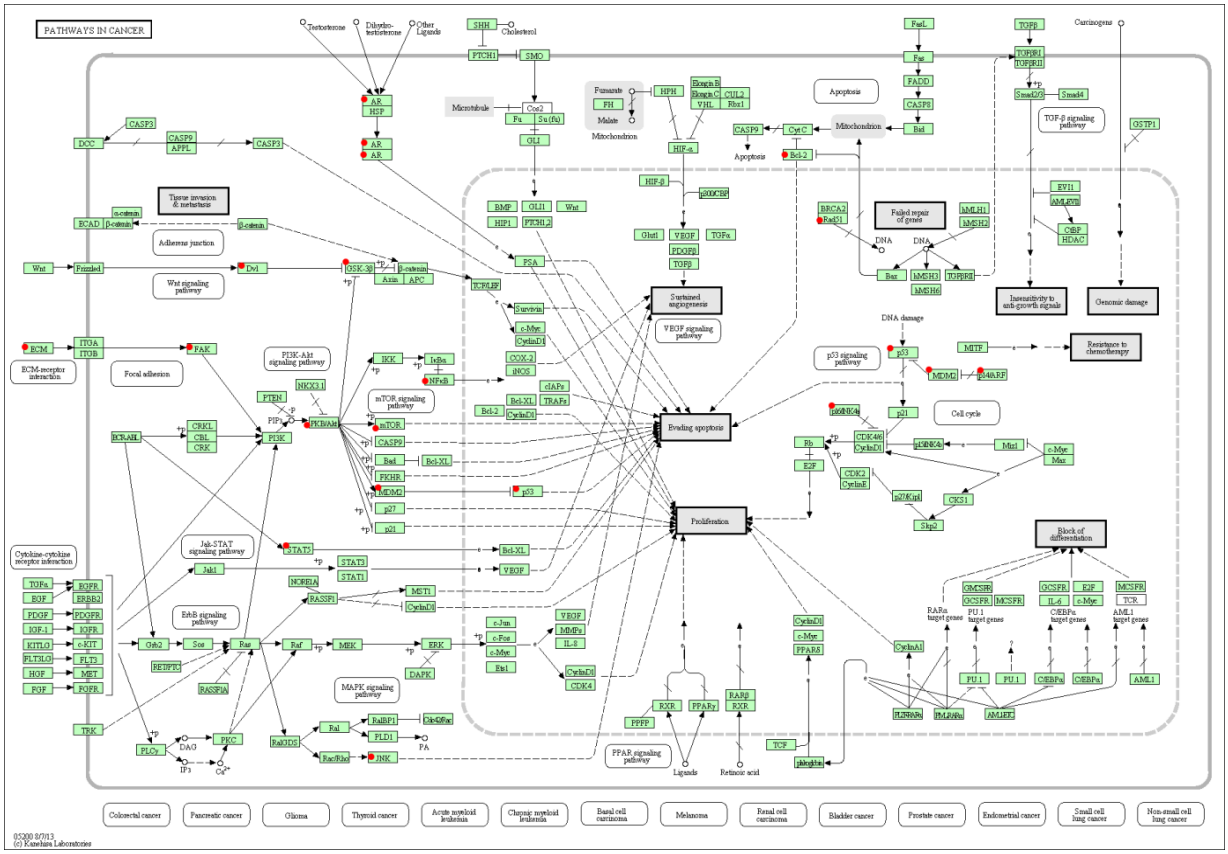

Figure 5: ACSL4 and pathways in cancer. Red marks highlight ACSL4-regulated genes in RPPA analysis. The pathway scheme was obtained from KEGG_PATHWAY database. Analysis was performed by DAVID bioinformatic tool.

stimulated the phosphorylation the mTOR pathway as previously described [22]. In accordance with the results mentioned above, ACSL4 overexpression also stimulates the expression of caveolin. Caveolin-1 is a ubiquitously expressed scaffolding protein which is enriched in caveolae –i.e. subtypes of lipid rafts– and which is involved in several cellular functions such as endocytosis, vesicular transport and signal transduction. Studies also revealed that caveolin-1 is an essential regulator of the invadopodia-mediated degradation of extracellular matrix, which indicates that caveolin-1 plays an essential role in cancer cell invasion [27]. Indeed, at least in breast cancer cell lines, caveolin-1 expression is predominantly observed in invasive cell lines and well correlated with invadopodia activity. These results correlate with those obtained in RNA-Seq, where cell movement showed the highest score (Table 3). Glycogen synthase kinase-3 alpha and beta (GSK3α and GSK3β), critical negative regulators of diverse signaling pathways, are two additional phosphoproteins whose levels exhibit an important increase in response to ACSL4 overexpression, and whose phosphorylation on Ser21 and Ser9, respectively, inhibits GSK3 activity. GSK3 has also been implicated in the negative regulation of FAK (focal adhesion kinase) activity [28]. As GSK3α has been shown to inhibit the Wnt signaling pathway, the inhibition of GSK3α activity by phosphorylation might suggest that Wnt signaling is part of the mechanism of action of ACSL4 overexpression. The aberrant regulation of the Wnt signaling pathway is a prevalent theme in cancer biology. From early observations that Wnt overexpression could lead to malignant transformation of mouse mammary tissue to the most recent genetic discoveries gleaned from tumor genome sequencing, the Wnt pathway continues to evolve as a central mechanism in cancer biology. Results from RNA-Seq also show that ACSL4 overexpression causes a strong reduction in the expression of *WIF1*. The protein encoded by this gene inhibits Wnt proteins, which are extracellular signaling molecules playing a role in embryonic development. Mammary cancer is a prominent example involving the Wnt pathway, particularly cancers classified as basal-like or triple-negative [29,30] which characteristically involve the expression of Wnt receptor FZD7 [31]. Accordingly, Yang et al. recently reported experiments in which knockdown of FZD7, in cell line models of triple-negative breast cancer, reduced the expression of Wnt target genes, inhibited tumorigenesis *in vitro* and greatly retarded the capacity of the MDA-MD-231 cell line to form tumors in mice [32]. These results suggest that Wnt ligands might drive certain breast cancers and are consistent with previous work from the Hynes laboratory [33]. In agreement with these data, ACSL4 overexpression increased the expression of *WNT6* and *WNT10A* (Figure 1). The *WNT6* gene is overexpressed in cervical cancer cell lines and strongly coexpressed with another family member, *WNT10A*, in a colorectal cancer cell line. *WNT6* overexpression may play a key role in carcinogenesis and is clustered with *WNT10A* in chromosome 2q35 region. The Wnt pathway is also implicated in the activation of mTORC1 through TSC1/2. In our studies, Wnt signaling inhibited GSK3β, which normally phosphorylates and promotes TSC2 activity, and ACSL4 overexpression produced the stimulation of GSK3 on Ser9, which suggests that this mechanism of mTORC1 activation is also used by ACSL4 [22]. As mentioned above, ACSL4 overexpression increases the phosphorylation of GSK3α and β, and a requirement for ACSL4 has recently been demonstrated in dorsoventral pattering of zebrafish embryo [12] and embryogenesis and neurogenesis in Drosophila [14,24]. These results show that ACSL4 works through the inhibition of AKT-dependent GSK3 activity by increasing its phosphorylation. And, given the interplay between morphogenic signals in developing

embryos, the interaction of these pathways might be expected in cancer. ACSL4 overexpression also stimulates the protein levels of growth factors and their receptors, such as the insulin-like growth factor binding protein (IGFBP2). Among genes involved in cell cycle control, ACSL4 decreases the level of the atalaxia telangiestasa (*ATM*) gene, a kinase that regulates cell cycle checkpoints by phosphorylating multiple proteins including histone H2AX, CHK1 and CHK2 kinases and p53. ATM is activated through auto- or transphosphorylation on Ser1981 and/or Ser1893 in response to DNA damage, particularly the induction of DNA double-strand breaks. ACSL4 also produces a substantial increase in cyclin-B1, the oncogen E3 ubiquitin protein ligase (MDM2), the eukaryotic translation factor 4E binding protein 1 (EEF2) and the GRB2-associated binding protein 2 (GAB2). In the energy area, genes regulated are the acetyl-CoA-carboxylase alpha and beta (*ACC*) and the succinate dehydrogenase complex subunit a flavoprotein (*SDHA*), a part of the respiratory chain. ACC participate in fatty acid synthesis and oxidation and are phosphorylated by AMP-activated protein kinase (AMPK) on Ser79 to inhibit their activity. ACSL4 overexpression decreases the activity of AMPK and thus decreases the phosphorylation of ACC. Finally, another gene increased by ACSL4 is the disheveled segment polarity protein 3 (*DVL3*), a member of a multi-gene family which bears strong similarities with the Drosophila disheveled gene, which in turn encodes a cytoplasmic phosphoprotein that regulates cell proliferation. The idea of personalized medicine and molecular profiling for prognostic tests has led to a plethora of studies in the past 10 years, in search for genetic determinants of metastasic breast cancer. Such studies have identified gene sets, or "signatures", whose expression in primary tumors is associated with higher risk of metastasis and poor disease outcome for the patients. Current views on cancer cell mutations hold that there are two different types: driver mutations, which are behind cancer growth because they give tumor cells a growth advantage, and passenger mutations, which are just along for the ride. It has been suggested that ACSL4 overexpression is led by a driver mutation [18,34]; however, as it is capable *per se* of changing cancer cell phenotypes, ACSL4 overexpression may be thought of as a backseat driver factor which generates changes in gene expression and signaling pathways toward a highly aggressive phenotype, and which acts in addition to passenger mutations when the driver gene is mutated. In summary, this study derives an ACSL4 overexpression gene and functional proteomic signature which might reveal important information about novel mediators of breast cancer cell aggressiveness. Here we report that ACSL4 overexpression can trigger several different mechanisms to regulate the aggressiveness of breast cancer cells, including the pathways stimulated by growth factors, nutrients, cytokines and changes in energy metabolism. The major findings of the present study are: (a) ACSL4 overexpression induces changes in genes associated with tumorigenesis-related biofunctions; (b) the four biofunctions with the highest activation z-scores are: cell movement, growth and proliferation, protein and cell assembly and organization; (c) the inhibition of ACSL4 expression completely abolishes the changes observed in protein expression and phosphorylation-dephosphorylation, which demonstrates the specificity of ACSL4 function; (d) since ACSL4 is *per se* capable of changing cancer cell phenotype, this protein overexpression may be thought of as a backseat driver factor which generates changes in gene expression and signaling pathways toward a highly aggressive phenotype; e) as ACSL4 has been related to colon and hepatocellular carcinoma, besides breast carcinoma, the present findings suggest novel mediators, specifically for combined pharmacological treatment toward tumor growth inhibition. Altogether, the present results open the possibility to use the inhibition of ACSL4 as a therapeutic tool in combination with agents targeting key molecular elements involved in breast cancer. In addition, ACSL4 could be used as a predictive marker that may provide the basis for patient therapy.

Acknowledgements

We thank Cristina Paz for her critical reading of the manuscript and María M. Rancez for providing language help and writing assistance. This work was supported by CONICET (PIP 2012-2014 - COD 11220110100485), Podesta; UBA (UBACYT 2011-2014 – 2002 0100100 849), Podesta.

References

1. Jemal A, Siegel R, Ward E, Murray T, Xu J, et al. (2007) Cancer statistics. CA Cancer J Clin 571: 43-66.
2. Monaco ME, Creighton CJ, Lee P, Zou X, Topham MK, et al. (2010) Expression of Long-chain Fatty Acyl-CoA Synthetase 4 in Breast and Prostate Cancers Is Associated with Sex Steroid Hormone Receptor Negativity. Transl Oncol 32: 91-98.
3. Maloberti PM, Duarte AB, Orlando UD, Pasqualini ME, Solano AR, et al. (2010) Functional interaction between acyl-CoA synthetase 4, lipooxygenases and cyclooxygenase-2 in the aggressive phenotype of breast cancer cells. PLoS One 511: e15540.
4. Orlando UD, Garona J, Ripoll GV, Maloberti PM, Solano AR, et al. (2012) The functional interaction between Acyl-CoA synthetase 4, 5-lipooxygenase and cyclooxygenase-2 controls tumor growth: a novel therapeutic target. PLoS One 77: e40794.
5. Wu X, Li Y, Wang J, Wen X, Marcus MT, et al. (2013) Long chain fatty Acyl-CoA synthetase 4 is a biomarker for and mediator of hormone resistance in human breast cancer. PLoS One 810: e77060.
6. Kang MJ, Fujino T, Sasano H, Minekura H, Yabuki N, et al. (1997) A novel arachidonate-preferring acyl-CoA synthetase is present in steroidogenic cells of the rat adrenal, ovary, and testis. Proc Natl Acad Sci U S A 947: 2880-2884.
7. Soupene E, Kuypers FA (2008) Mammalian long-chain acyl-CoA synthetases. Exp Biol Med (Maywood) 2335: 507-521.
8. Watkins PA, Ellis JM (2012) Peroxisomal acyl-CoA synthetases. Biochim Biophys Acta 18229: 1411-1420.
9. Watkins PA (1997) Fatty acid activation. Prog Lipid Res 361: 55-83.
10. Li LO, Klett EL, Coleman RA (2010) Acyl-CoA synthesis, lipid metabolism and lipotoxicity. Biochim Biophys Acta 18013: 246-251.
11. Cao Y, Murphy KJ, McIntyre TM, Zimmerman GA, Prescott SM (2000) Expression of fatty acid-CoA ligase 4 during development and in brain. FEBS Lett 4672-3: 263-267.
12. Miyares RL, Stein C, Renisch B, Anderson JL, Hammerschmidt M, et al. (2013) Long-chain Acyl-CoA synthetase 4A regulates Smad activity and dorsoventral patterning in the zebrafish embryo. Dev Cell 276: 635-647.
13. Maloberti P, Castilla R, Castillo F, Maciel FC, Mendez CF, et al. (2005) Silencing the expression of mitochondrial acyl-CoA thioesterase I and acyl-CoA synthetase 4 inhibits hormone-induced steroidogenesis. Febs J 2727: 1804-1814.
14. Y, Zhang Y, Gao Y, Zhao X, Wang Z (2011) Drosophila long-chain acyl-CoA synthetase acts like a gap gene in embryonic segmentation. Dev Biol 3532: 259-265.
15. Gazou A, Riess A, Grasshoff U, Schaferhoff K, Bonin M, et al. (2013) Xq22.3-q23 deletion including ACSL4 in a patient with intellectual disability. Am J Med Genet A 161A4: 860-864.
16. Modi HR, Basselin M, Taha AY, Li LO, Coleman RA, et al. (2013) Propylisopropylacetic acid (PIA), a constitutional isomer of valproic acid, uncompetitively inhibits arachidonic acid acylation by rat acyl-CoA synthetase 4: a potential drug for bipolar disorder. Biochim Biophys Acta 18314: 880-886.
17. Sung YK, Hwang SY, Park MK, Bae HI, Kim WH, et al. (2003) Fatty acid-CoA ligase 4 is overexpressed in human hepatocellular carcinoma. Cancer Sci 945: 421-424.
18. Cao Y, Dave KB, Doan TP and Prescott SM (2001) Fatty acid CoA ligase 4 is up-regulated in colon adenocarcinoma. Cancer Res 6123: 8429-8434.
19. Jiang M, Huang O, Xie Z, Wu S, Zhang X, et al. (2014) A novel long non-coding RNA-ARA: adriamycin resistance-associated. Biochem Pharmacol 872: 254-283.
20. Database for Annotation, Visualization and Integrated Discovery (DAVID) http://david.abcc.ncifcrf.gov.
21. Ingenuity Pathways Analysis (IPA). http://www.ingenuity.com.

22. Orlando UD, Castillo AF, Dattilo MA, Solano AR, Maloberti PM, et al. (2015) Acyl-CoA synthetase-4, a new regulator of mTOR and a potential therapeutic target for enhanced estrogen receptor function in receptor-positive and -negative breast cancer. Oncotarget In press.

23. Pignatelli M, Serras F, Moya A, Guigo R, Corominas M (2009) CROC: finding chromosomal clusters in eukaryotic genomes. Bioinformatics 2512: 1552-1553.

24. Liu Z, Huang Y, Hu W, Huang S, Wang Q, et al. (2014) dAcsl, the Drosophila ortholog of acyl-CoA synthetase long-chain family member 3 and 4, inhibits synapse growth by attenuating bone morphogenetic protein signaling via endocytic recycling. J Neurosci 348: 2785-2796.

25. Endo Y, Toyama T, Takahashi S, Yoshimoto N, Iwasa M, et al. (2013) miR-1290 and its potential targets are associated with characteristics of estrogen receptor alpha-positive breast cancer. Endocr Relat Cancer 201: 91-102.

26. Johnson CD, Esquela-Kerscher A, Stefani G, Byrom M, Kelnar K, et al. (2007) The let-7 microRNA represses cell proliferation pathways in human cells. Cancer Res 6716: 7713-7722.

27. Yamaguchi H, Takeo Y, Yoshida S, Kouchi Z, Nakamura Y, et al. (2009) Lipid rafts and caveolin-1 are required for invadopodia formation and extracellular matrix degradation by human breast cancer cells. Cancer Res 6922: 8594-8602.

28. Golubovskaya VM (2010) Focal adhesion kinase as a cancer therapy target. Anticancer Agents Med Chem 1010: 735-741.

29. Geyer FC, Lacroix-Triki M, Savage K, Arnedos M, Lambros MB, et al. (2011) beta-Catenin pathway activation in breast cancer is associated with triple-negative phenotype but not with CTNNB1 mutation. Mod Pathol 242: 209-231.

30. Khramtsov AI, Khramtsova GF, Tretiakova M, Huo D, Olopade OI, et al. (2010) Wnt/beta-catenin pathway activation is enriched in basal-like breast cancers and predicts poor outcome. Am J Pathol 1766: 2911-2920.

31. Sorlie T, Tibshirani R, Parker J, Hastie T, Marron JS, et al. (2003) Repeated observation of breast tumor subtypes in independent gene expression data sets. Proc Natl Acad Sci U S A 10014: 8418-8423.

32. Yang L, Wu X, Wang Y, Zhang K, Wu J, et al. (2011) FZD7 has a critical role in cell proliferation in triple negative breast cancer. Oncogene 3043: 4437-4446.

33. Matsuda Y, Schlange T, Oakeley EJ, Boulay A, Hynes NE (2009) WNT signaling enhances breast cancer cell motility and blockade of the WNT pathway by sFRP1 suppresses MDA-MB-231 xenograft growth. Breast Cancer Res 113: R32.

34. Kaller M, Liffers ST, Oeljeklaus S, Kuhlmann K, Roh S, et al. (2011) Genome-wide characterization of miR-34a induced changes in protein and mRNA expression by a combined pulsed SILAC and micro-array analysis. Mol Cell Proteomics.